PHYSICAL REVIEW B VOLUME 21, NUMBER 10 15 MAY 1980

Photoemission from alkali halides: Energies and line shapes

G. D. Mahan
Physics Department, Indiana University, Bloomington, Indiana 47405
(Received 16 May 1979)

Energies and line shapes are calculated for photoemitted electrons from core and valence states in alkali halides. Energies are obtained by assuming that the holes are localized at lattice points and by using the point-ion model. The usual energy terms are obtained, including the ionization potential of the free ion, the Madelung energy, and the Mott-Littleton relaxation energy. An exact solution of the point-ion model is presented, which derives a new energy term from relaxation. The inclusion of this term considerably improves the agreement between theory and experiment for threshold energies. In addition, the phonon relaxation energy and line shapes are calculated for ten salts.

I. INTRODUCTION

The alkali halides form a class of 20 solids which have been often studied in photoemission.[1-7] There have been many measurements of valence band energies, line shapes, and conduction-band structure. The object of the present calculation is to determine the absolute value, relative to the vacuum energy, of the energies of hole states in the valence and core states. We report a new contribution to the relaxation energy, heretofore overlooked, in addition to the traditional terms of Madelung and Mott-Littleton.[8] We also wrote a computer code to describe phonon states in ten of these salts, and used it to obtain the phonon relaxation energy and phonon contribution to the photoemission linewidth. Citrin *et al.*[7] showed that this was the dominant linewidth contribution, and we agree well with their experimental results.

We adopt the traditional model that the holes in the valence and core states are localized.[1,2,7,8] Then the energy to create the hole can be calculated by taking the ionization potential of the free ion, and adding it to the additional potential energy terms that the hole has in the crystal. The point-ion model is adopted for the crystal, so that all potential energy terms, such as Madelung energies, can be calculated by Ewald summations. In Sec. II we start from the exact equation for the potential energy in the point-ion model, and derive the exact expression for the energy shift between the free ion and crystal. We find the traditional terms of Madelung and the relaxation energy of Mott-Littleton.[8] In addition, a new term is found which derives from the relaxation energy. It is actually the difference of two terms, of which one is the screening of the Madelung energy, while the second is another self-interaction term twice that of Mott-Littleton. They largely cancel, and the resulting term can have either sign, and has a typical magnitude of 1 eV. When it is included in the calculation of threshold energies, there is considerable improvement when comparing to experiment. Our calculation of the Mott-Littleton energy is more accurate than recent workers.[1,2] We express it exactly as an integral over the Brillouin zone in wave-vector space, and evaluate this integral accurately by the method of special-points integration.[9]

The localized-hole, point-ion model has previously been used with great success to describe the photoemission in the alkali halides. Citrin and Thomas[1] measured 14 different solids and compared results with the point-ion model. They include a repulsive term which we find unconvincing and choose to omit. They made the important experimental observation that different holes on the same ion have the same energy shifts in the crystal. For example, a hole on the Cl^- ion has the same change of threshold energy, relative to the free ion, regardless as to whether the hole is in the $1s$ or $3p$ state. They interpret this as positive evidence that the holes are all localized, even in the upper valence band. Surely the holes are localized for core states, so they argue convincingly that the valence band hole is also localized if it has the same self-energy.

One would also expect the valence holes would be localized on theoretical grounds. Polaron theory shows that the hole will become localized whenever the polaron constant exceeds about 6. The narrow valence bandwidths[10] found for occupied valence states predicts a hole band mass which is quite large. This large mass, and the polar nature of these salts, results in large values of the polaron coupling constant, which would imply a trapped or localized hole state. Thus theory and experiment seem to agree that valence holes are localized in most alkali halides. There is experimental evidence to the contrary in several cases, such as the valence band structure in NaCl and LiCl found by Pong and Smith,[5] but these seem to be exceptions to the general behavior.

Further evidence for the localized-hole, point-

ion model was found by Poole *et al.*[2] They measured hole energies in 18 alkali halides, and compared results with the model. They investigated the quantity $E_s^{expt} = E_b^{expt}(A^+) - E_b^{expt}(H^-)$ which is the difference between the experimental binding energies for the hole on the alkali and halide ions. The virtue of studying this quantity is that it is free of the influence of surface effects such as a dipole layer.[11] They found that the experimental values of E_s^{expt} are well described by the localized-hole, point-ion (LHPI) model. The predictions of this model are

$$E_s^{th} = E_b^{fi}(A^+) - E_b^{fi}(H^-) - 2E_M - \Sigma_{ML}(A^+) + \Sigma_{ML}(H^-)$$

which is the difference of the free-ion binding energies, minus twice the Madelung energy E_M, and minus the difference in the Mott-Littleton relaxation energies for the hole in the alkali and halide ions. They found excellent agreement between theory and experiment for E_s among the 12 crystals they could measure.

The additional relaxation energy term we find in Sec. II has the same value for the hole in the alkali or halide ion. Thus it cancels out in the quantity E_s, and does not disturb this agreement between theory and experiment.

All of the above terms are associated with relaxation energies from electronic polarization and dielectric screening. The ions can also move, and readjust their position in response to the core-hole potential. This can be determined by solving for the hole-phonon interaction $M_\lambda(q)$, and using it to find the hole self-energy from phonons, and the contribution to the observed linewidths in photoemission. The theory for this is identical to the Huang-Rhys model for the F center,[12] and was applied to the core-level spectroscopy by Parratt and Overhauser.[13] Citrin, Eisenberger, and Hamann (CEH) (Ref. 7) provided detailed measurements of the phonon contribution to the linewidth as a function of temperature, and showed that a simple model gave qualitative agreement with experiment. We have tested the model further by doing a complete phonon calculation which sums over all six modes λ (TA, LA, TO, LO) and over the Brillouin zone in wave-vector space. The coupling is quite strong, in which case the phonon self-energy and linewidth [full width at half maximum (FWHM)] are given by $\beta = 1/k_B T$ (Refs. 12–15)

$$\Sigma_{ph} = \sum_\lambda \int \frac{d^3q}{(2\pi)^3} \frac{|M_\lambda(q)|^2}{\hbar\omega_\lambda(q)}, \tag{1}$$

$$\Delta(T) = 2.35\left(\sum_\lambda \int \frac{d^3q}{(2\pi)^3} |M_\lambda(q)|^2 \coth[\beta\hbar\omega_\lambda(q)/2]\right)^{1/2}. \tag{2}$$

The details of this calculation are given in Sec. III. The only experimental test which can be made so far is with the linewidth, and our results agree favorably with the two cases reported by CEH for which we were able to do calculations.

The self-energy Σ_{ph} from phonons is calculated for 10 alkali halides, and the numbers are typically between 1 and 2 eV. This represents a large contribution to the hole energy—of the same order as the Mott-Littleton energy—but this large value does not affect the core binding energy as observed in photoemission. This statement may appear surprising, but is a natural consequence of strong coupling theory. This is illustrated in Fig. 1. The energy level E_b is calculated using all of the electronic contributions to relaxation such as Mott-Littleton and the one we report in Sec. II, but not phonons. The absorption of a photon of energy $\hbar\omega$ may cause an electron to leave the solid, where it has an external kinetic energy of E_{KE}. A measurement of this kinetic energy permits the deduction of $E_b = \hbar\omega - E_{KE}$.

The inclusion of phonons results in a different picture of the photoemission, as shown in the right in Fig. 1.[12-15] First, the hole self-energy $-\Sigma_{ph}$ from (1) lowers the hole energy, which moves it closer to the vacuum. This lowers the threshold for photoemission. Now the absorption of a photon of energy $\hbar\omega$ could take an electron to the dashed line, which has a higher external kinetic energy. However, the probability of this no-phonon transition is negligible in strong coupling. Instead, many phonons are produced when making the hole. The energy to do this is subtracted from

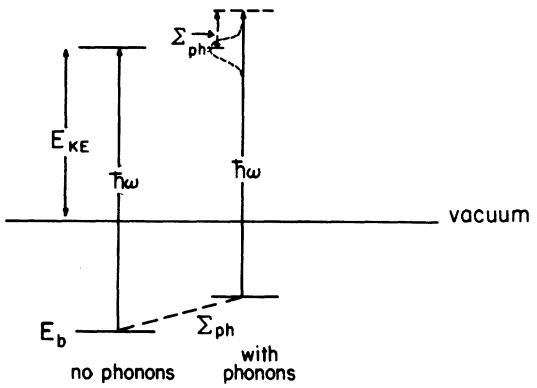

FIG. 1. On the left is illustrated an electronic energy level at E_b. When it absorbs a photon with energy $\hbar\omega$, the external electron has kinetic energy E_{KE}. The inclusion of phonons lowers the binding energy by the hole self-energy Σ_{ph}. Phonons also impart a Gaussian line shape to the distribution of emitted electrons. The peak of this Gaussian has the same external kinetic energy E_{KE} as expected in the absence of phonon processes.

that imparted to the electron, so that it has on the average much less external kinetic energy. The theory shows that the resulting line shape is Gaussian, and the peak of the Gaussian is shifted to lower kinetic energy by the same self-energy Σ_{ph}. Thus, the peak in the photoemission occurs at an external kinetic energy which is identical to that without the phonon self-energy. Thus the quantity Σ_{ph} can not be directly deduced from these experiments unless one can observe the no-phonon line, which is unlikely in alkali halides. The important experimental number for comparison is the peak position, which can be compared directly to the binding energy predicted from just the electronic component of the hole energy. This is what we shall do when comparing with experiments. Both Poole *et al.*[2] and Pong *et al.*[3-6] report peak energies of $p_{3/2}$ holes and we deduced them from Citrin and Thomas[1] by taking their values for the midpoint of the p band and subtracting one-half of the spin-orbit splitting of the band. The final core-hole energy is deduced by subtracting Σ_{ph} from the electronic contributions. These lines are usually found to be Gaussian, which is a further confirmation of the model. Many experimentalists report the threshold energy. This is now regarded as a useless quantity, since it is a description of where the tail begins in the Gaussian, which is ill defined. The procedure we advocate seems much simpler: to use the peak in the emission as a measurement of the electronic contributions to the hole energy, and then to calculate the phonon part theoretically. The simultaneous calculation of the linewidth, as a function of temperature, provides a test of the phonon calculation.

We adopt the convention that energy symbols such as E_M, Σ_{ML}, Σ_{ph} refer to positive quantities, so a negative relaxation energy becomes $-\Sigma_{ph}$. The exception to this is the new term we derive in Sec. II which is called Σ_2 because its sign varies from solid to solid. Since we are talking about hole states, lowering its energy moves the core level closer to the vacuum and lowers the threshold for photoemission.

II. ELECTRONIC RELAXATION

This section derives the electronic contribution to the hole energies, while the phonon energies are discussed in the following section. Here we treat the ions as fixed on their lattice sites. In the LHPI model we assign each ion a charge q_j and polarizability $\underline{\alpha}_j$ at site $\vec{R}_j$. The hole has a classical potential energy from interacting with these polarizable point charges, which also interact among themselves. The threshold energy in photoemission is given in this model as

$$E_b = E_{IP} + E_{elec} ,$$

where E_{elec} is a positive quantity for halide holes and a negative quantity for alkali holes. The first term E_{IP} is the ionization potential of the free ion. For cation holes we use values from Moore,[16] while for the electron affinity of halide ions we use Berry and Reimann.[17] Our immediate goal is to calculate E_{elec}.

An expression was given previously for the ground-state energy of an interacting system of polarizable point charges[18]

$$E_g = \tfrac{1}{2}{\sum_{ij}}' \frac{q_i q_j}{R_{ij}} - \tfrac{1}{2} \sum_{ijm,\, m\neq ij} q_i q_j \left(\vec{w}(\vec{R}_{im}) \cdot \underline{\alpha}_m \cdot \vec{w}(\vec{R}_{jm}) - \sum_n \vec{w}(\vec{R}_{im}) \cdot \underline{\alpha}_m \cdot \underline{\phi}(\vec{R}_{mn}) \cdot \underline{\alpha}_n \cdot \vec{w}(\vec{R}_{ij}) + \cdots \right) ,$$

$$w_\mu(R) = R_\mu / R^3 , \tag{3}$$

$$\phi_{\mu\nu}(R) = \delta_{\mu\nu}/R^3 - 3R_\mu R_\nu / R^5 .$$

The summation over ij includes each pair twice. This is a general result which is valid for any arrangement of ions. We shall specialize to the case that the ions are either of type A or B on a cubic binary lattice. First take the situation where the lattice is ideal and has no holes. Then the polarization terms average to zero, and the ground-state energy is just the Madelung term

$$E_g = -N e^2 \alpha / 2a ,$$

where α is the Madelung constant and a is the lattice constant. Next we consider the addition of a hole to any site, which we take to be the origin. The hole results in a change in charge $q_0 \to q_0 + \delta q$, polarizability $\underline{\alpha}_0 \to \underline{\alpha}_0 + \underline{\delta}\alpha$ and ground-state energy $E_g \to E_g + \delta E_g$. We ignore the effect of this change in polarizability since our estimates show this to be a small contribution to the energy change $\delta E_g \equiv E_{elec}$. Thus we want the change in ground-state energy from the change in charge δq, which is positive for a hole

$$E_{\text{elec}} \equiv \delta E_g = \delta q \sum_j{}' \frac{q_j}{R_{0j}} - \tfrac{1}{2}(\delta q)^2 \sum_m \Big(\vec{w}(\vec{R}_{0m}) \cdot \underline{\alpha}_m \cdot \vec{w}(\vec{R}_{0m}) - \sum_n \vec{w}(\vec{R}_{0m}) \cdot \underline{\alpha}_m \cdot \underline{\phi}(\vec{R}_{mn}) \cdot \underline{\alpha}_n \cdot \vec{w}(\vec{R}_{0n}) + \cdots \Big)$$

$$- \delta q \sum_{jm,\, m \neq j} q_j \Big(\vec{w}(\vec{R}_{0m}) \cdot \underline{\alpha}_m \cdot \vec{w}(\vec{R}_{jm}) - \sum_n \vec{w}(\vec{R}_{0m}) \cdot \underline{\alpha}_m \cdot \underline{\phi}(\vec{R}_{mn}) \cdot \underline{\alpha}_n \cdot \vec{w}(\vec{R}_{jn}) + \cdots \Big) . \tag{4}$$

These energy terms will be evaluated one by one, according to their traditional definitions.

The Madelung energy term is the largest. It is given by

$$\pm E_M = \delta q \sum_{j \neq 0} \frac{q_j}{R_{0j}} = \delta q \, \frac{q_B}{a} \alpha . \tag{5}$$

We adopt the convention that the hole is on the A sublattice, and A or B subscripts refer to quantities on the two sublattices $q_A = -q_B$. For halide holes q_B and the Madelung energy are both positive, while both are negative for cation holes.

The next set of terms we consider are

$$\Sigma_{\text{ML}} = \tfrac{1}{2}(\delta q)^2 \sum_m \Big(\vec{w}(\vec{R}_{0m}) \cdot \underline{\alpha}_m \cdot \vec{w}(\vec{R}_{0m}) - \sum_n \vec{w}(\vec{R}_{0m}) \cdot \underline{\alpha}_m \cdot \underline{\phi}(\vec{R}_{mn}) \cdot \underline{\alpha}_m \cdot \vec{w}(\vec{R}_{0n}) + \cdots \Big) . \tag{6}$$

Here the physics is quite simple: the hole polarizes the medium, and this polarization acts back upon the hole. Of course, this is the famous energy term first considered by Mott and Littleton,[8] and has been evaluated by a number of workers. We have developed a rather accurate method of evaluating this contribution, which we shall now describe. It consists of changing the summations in real space into summations in wave vector space. This permits a simple summation of the series of many interaction terms. There remains only an integration over the Brillouin zone, which is easily done using the method of special points.[9]

The first step in the evaluation of Σ_{ML} is to define some lattice transforms of various Coulomb interactions. For a binary lattice, we need to define one quantity with an "e" superscript for the summation over equivalent lattice sites such as AA and BB. Another quantity with an "i" superscript is for summations over interactions between the A and B sublattices.[19]

$$W^e_\mu(k) = \frac{V_0}{4\pi} \sum_{\vec{l}}{}' e^{i\vec{k}\cdot\vec{l}} w_\mu(l) ,$$

$$W^i_\mu(k) = \frac{V_0}{4\pi} \sum_{\vec{l}} e^{i\vec{k}\cdot(\vec{l}-\vec{l}_0)} w_\mu(\vec{l} - \vec{l}_0) ,$$

$$T^e_{\mu\nu} = \frac{V_0}{4\pi} \sum_{\vec{l}}{}' e^{i\vec{k}\cdot\vec{l}} \phi_{\mu\nu}(\vec{l}) , \tag{7}$$

$$T^i_{\mu\nu} = \frac{V_0}{4\pi} \sum_{\vec{l}} e^{i\vec{k}\cdot(\vec{l}-\vec{l}_0)} \phi_{\mu\nu}(\vec{l} - \vec{l}_0) ,$$

where V_0 is the volume per unit cell, $\vec{l}$ are lattice vectors, and $\vec{l}_0$ is between the A and B sublattice. The atomic polarizabilities α_A and α_B are assumed to be isotropic, and multiples of the unit vector. We also introduce the symbols for the dimensionless polarizability:

$$\bar{\alpha}_A = 4\pi\alpha_A / V_0 ,$$

$$\bar{\alpha}_B = 4\pi\alpha_B / V_0 ,$$

$$\epsilon_\infty = 1 + (\bar{\alpha}_A + \bar{\alpha}_B)/[1 - \tfrac{1}{3}(\bar{\alpha}_A + \bar{\alpha}_B)] .$$

In terms of these quantities, the summations over real space in (6) can be replaced by summations over reciprocal space. Since the real-space summations go over both A and B sublattices, there are many combinations of terms

$$\Sigma_{\text{ML}} = \tfrac{1}{2}(\delta q)^2 \frac{4\pi}{V_0 N} \sum_{\vec{k}} \{ \bar{\alpha}_A \vec{W}^e(k) \cdot \vec{W}^e(k)^* + \bar{\alpha}_B \vec{W}^i(k) \cdot \vec{W}^i(k)^* - \bar{\alpha}_A^2 \vec{W}^e(k) \cdot \underline{T}^e \cdot \vec{W}^e(k)^*$$

$$- \bar{\alpha}_B^2 \vec{W}^i(k) \cdot \underline{T}^e(k) \cdot \vec{W}^i(k)^* - \bar{\alpha}_A \bar{\alpha}_B [\vec{W}^e(k) \cdot \underline{T}^i \cdot \vec{W}^{i\,*} + \vec{W}^i \cdot \underline{T}^i \cdot \vec{W}^{e*}] + \cdots \} . \tag{8}$$

These many terms express the physics that the hole charge is polarizing the various ions, which in turn polarize other ions. The summation of all possibilities is given by the above series. It is really just the inclusion of dielectric screening. The terms in this series may be summed by defining $\vec{J}_{NM}(\vec{k})$ as the

potential acting upon site M due to an initial polarization on site N. There are four possible terms $\vec{J}_{AA}$, $\vec{J}_{BB}$, $\vec{J}_{AB}$, $\vec{J}_{BA}$, and two of them obey the coupled equations

$$\begin{aligned}\vec{J}_{AA}(\vec{k}) &= \vec{W}^e(\vec{k}) - \bar{\alpha}_A \underline{T}^e(\vec{k}) \cdot \vec{J}_{AA}(\vec{k}) - \bar{\alpha}_B \underline{T}^i(\vec{k}) \cdot \vec{J}_{BA}(\vec{k}) , \\ \vec{J}_{BA}(\vec{k}) &= \vec{W}^i(\vec{k}) - \bar{\alpha}_B \underline{T}^e(\vec{k}) \cdot \vec{J}_{BA}(\vec{k}) - \bar{\alpha}_A \underline{T}^i(\vec{k}) \cdot \vec{J}_{AA}(\vec{k}) .\end{aligned} \tag{9}$$

When these equations are iterated, they produce a series of terms which are recognized as the same ones in Eq. (8). So the Mott-Littleton relaxation energy can be expressed as

$$\Sigma_{ML} = \tfrac{1}{2}(\delta q)^2 \frac{4\pi}{NV_0} \sum_{\vec{k}} [\bar{\alpha}_A \vec{W}^e(\vec{k}) \cdot \vec{J}_{AA}(\vec{k})^* + \bar{\alpha}_B \vec{W}^i(\vec{k}) \cdot \vec{J}_{BA}(\vec{k})^*] . \tag{10}$$

This is an exact expression for this energy in the LHPI model.

This was evaluated numerically at a set of k points by first solving for the vector functions $\vec{W}^e(\vec{k})$ and $\vec{W}^i(\vec{k})$ and matrix functions $\underline{T}^e(\vec{k})$ and $\underline{T}^i(\vec{k})$ using Ewald techniques. The six-dimensional equations in (9) were solved for the vector functions $\vec{J}_{AA}$ and $\vec{J}_{BA}$, which were used to find the quantity in brackets in Eq. (10). The set of k points were selected by the method of special-points integration.[9] Here the summation over all of the N points in the Brillouin zone is approximated by a summation over a small set of selected points $\vec{k}_i$ with a weight factor a_i.

$$\frac{1}{N} \sum_{\vec{k}} f(\vec{k}) \simeq \sum_{\vec{k}_i} a_i f(\vec{k}_i) .$$

It is required that $f(\vec{k})$ be periodic in $\vec{k}$, which is satisfied in our case. As described in Ref. 9, these k points and weights are selected on the premise that the lattice transform of $f(\vec{k})$

$$F(\vec{R}) = \frac{1}{N} \sum_{\vec{k}} e^{i\vec{k}\cdot\vec{R}} f(\vec{k})$$

converges rapidly in R space. The integral in (10) which we are evaluating is a Coulomb potential $F(R) \sim R^{-1}$ at large distance, which is one of the least rapidly converging functions one could contemplate. In order to speed up convergence, we instead evaluated

$$\sum_i a_i [f(\vec{k}_i) - V(\vec{k}_i)(1 - 1/\epsilon_\infty)] ,$$

$$V(\vec{k}) = \frac{4\pi}{V_0} \sum_{\vec{l}\neq 0} e^{i\vec{k}\cdot\vec{l}} \frac{1}{l} .$$

The function $V(\vec{k})$ is selected to cancel the k^{-2} term in $f(\vec{k})$ in the limit of $k \to 0$, so the net $F(\vec{R})$ is now a rapidly converging function, but the Brillouin zone integral of $V(\vec{k})$ is zero. So we are adding a zero to the result, but one which makes the special-points method converge rapidly. For the fcc Brillouin zone of the rocksalt lattice, increasing accuracy is obtained by using sets with the increasing number of points 2, 10, 60, etc. Our calculations showed that going from 2 to 10 points changed the k summations by 1.5%, while the change from 10 to 60 changed the result by only 0.15%. We assume this convergence indicates the degree of accuracy, so a 10-point set gives 0.2% accuracy while the 60-point set does much better. All of the Mott-Littleton and phonon energies we report were done with the 60-point set. We find it truly amazing that the 2-point set has an accuracy of 2%.

In order to compare with other recent evaluations of the Mott-Littleton relaxation energy, it is fair to use the same data set. Citrin and Thomas[1] used the polarizabilities of Tessman, Kahn, and Shockley (TKS),[20] while Poole *et al.*[2] used those of Jaswal and Sharma (JS).[21] These results and comparisons are shown in Table I for both halide and cation holes. The present results differ from the previous results by 1–20%, and we expect our numbers are accurate to better than 0.1%. Probably the most accurate previous evaluation of the Mott-Littleton energy was by DuPré *et al.*[22] whose results are not used because of their old-fashioned choice of atomic polarizabilities. We check our method by doing the calculation with their data set, and found we agreed with them with an error of 0.5 to 1%. A quite different method of calculating this relaxation energy was done by Kunz,[10] who sums over the real band structure of the solid, but includes the dielectric screening in an approximate way. His approach is necessary in those cases where the hole is not localized.

So far two of the energy terms in (4) have been evaluated. The remaining term is called Σ_2, and has the same value for halide or cation holes.

$$\begin{aligned}E_b(H^-) &= E_{IP} + E_M - \Sigma_{ML}(H^-) - \Sigma_2 , \\ E_b(A^+) &= E_{IP} - E_M - \Sigma_{ML}(A^+) - \Sigma_2 , \\ E_{elec}(H^-) &= E_M - \Sigma_{ML}(H^-) - \Sigma_2 , \\ E_{elec}(A^+) &= -E_M - \Sigma_{ML}(A^+) - \Sigma_2 .\end{aligned} \tag{11}$$

The necessity for additional terms like Σ_2 in the LHPI model can be understood by an intuitive argument which provided the motivation for the

TABLE I. Mott-Littleton energies (eV).

	Halide hole				Alkali hole			
	TKS[a]		JS[b]		TKS[a]		JS[b]	
Salt	Present	Citrin[c]	Present	Poole[d]	Present	Citrin[c]	Present	Poole[d]
LiF	1.656		1.800	1.78	2.644		2.894	2.94
LiCl	1.916	1.82	1.906	1.82	3.202	3.19	3.184	3.21
LiBr	1.911		1.900	1.82	3.216		3.197	3.24
LiI	1.897		1.883		3.219		3.194	
NaF	1.441	1.58	1.585	1.58	1.846	1.86	2.032	2.06
NaCl	1.593	1.45	1.606	1.59	2.462	2.54	2.456	2.50
NaBr	1.618	1.47	1.625	1.59	2.566	2.60	2.556	2.59
NaI	1.612	1.47	1.611		2.621	2.69	2.603	
KF	1.776		1.759	1.79	1.585		1.641	1.67
KCl	1.543	1.58	1.510	1.53	1.920	1.94	1.898	1.94
KBr	1.518		1.491	1.51	2.021		2.000	2.05
KI	1.478		1.454	1.46	2.108		2.085	2.14
RbF	1.899		1.853	1.89	1.544		1.572	1.59
RbCl	1.550	1.61	1.506	1.55	1.760	1.76	1.734	1.78
RbBr	1.523		1.486	1.50	1.869		1.845	1.87
RbI	1.443		1.412	1.44	1.926		1.901	1.96
AgF	3.214		3.272		2.483		2.583	
AgCl	2.748		2.758		3.003		2.996	
AgBr	2.641		2.648		3.155		3.144	
CsF	2.201	2.24	2.044	2.08	1.604	1.45	1.561	1.57
CsCl	1.871	2.20	1.788	2.24	1.852	2.13	1.813	2.27
CsBr	1.807	1.99	1.740	2.16	1.902	2.05	1.874	2.31
CsI	1.698	1.90	1.654	2.04	1.919	2.11	1.908	2.35

[a] Polarizabilities from Tessman, Kahn, and Shockley, Ref. 20.
[b] Polarizabilities from Jaswal and Sharma, Ref. 21.
[c] Citrin and Thomas, Ref. 1.
[d] Poole *et al.*, Ref. 2.

present research. This is the observation that the Madelung energy term in (5) should be screened. Since we are considering the electronic contributions to the hole energy, it should be screened by the electronic contribution to the dielectric constant which is ϵ_∞. A static charge in the dielectric produces a potential field which is screened, so that one should have somewhere in the theory another term which is $-E_M(1-1/\epsilon_\infty)$ which when added to (5) gives E_M/ϵ_∞. Since E_M is typically 8–10 eV and $\epsilon_\infty \sim 2$–3, this produces a large contribution to the hole energy which has been previously overlooked. In fact, this term is contained in Σ_2. However, there is a second contribution in Σ_2 which is also large and has the opposite sign, so that the two largely cancel and the residue is much smaller and of variable sign.

From Eq. (4) the expression for Σ_2 is

$$\Sigma_2 = \delta q \sum_{j,m,\, m\neq j} q_j \Big(\vec{w}(\vec{R}_{0m}) \cdot \underline{\alpha}_m \cdot \vec{w}(\vec{R}_{jm}) - \sum_n \vec{w}(\vec{R}_{0m}) \cdot \underline{\alpha}_m \cdot \underline{\phi}(\vec{R}_{mn}) \cdot \underline{\alpha}_n \cdot \vec{w}(\vec{R}_{jn}) + \cdots \Big).$$

The summation over j includes all ion sites, even the one at $\vec{R}_0$ where the hole is located. For those sites with $\vec{R} \neq \vec{R}_0$, the terms do describe the screening of the Madelung energy, since they originate from the hole polarizing the medium. This polarization causes a potential which interacts with the charges on the other ions. This term can also be evaluated using wave-vector transforms,

$$\Sigma_2 = -q_B \delta q \frac{4\pi}{NV_0} \sum_{\vec{l},\vec{k}} e^{i\vec{k}\cdot\vec{l}} \{ \bar{\alpha}_A \vec{W}^e(\vec{k}) \cdot \vec{J}_{AA}(k)^* + \bar{\alpha}_B \vec{W}^i(\vec{k}) \cdot \vec{J}_{BA}(\vec{k})^* - e^{i\vec{k}\cdot\vec{l}_0} [\bar{\alpha}_A \vec{W}^e(\vec{k}) \cdot \vec{J}_{AB}(\vec{k})^* + \bar{\alpha}_B \vec{W}^i(\vec{k}) \cdot \vec{J}_{BB}(\vec{k})^*] \}. \quad (12)$$

Some terms in this series for $\vec{R}_j \neq \vec{R}_0$ were evaluated by special-point integration. They were found to equal the classical quantity $e^2(1-1/\epsilon_\infty)/R_j$ within 10% for neighboring lattice points and with less error for further points. The classical quantity is not rigorous because of the atomicity of the dielectric.[19] Nonetheless, the physics of these terms is clearly that of dielectric screening. There is also the term with $\vec{R}_j = \vec{R}_0$ which represents the hole polarizing the medium, and this polarization acting back upon the charge of the host ion. This is exactly twice the Mott-Littleton energy, and with a sign which causes it to largely cancel the screening of the Madelung energy. The resultant term Σ_2 is smaller than either of its two contributions.

Now that we have explained the physics of this self-energy term, we shall show it may be evaluated in a simple way. The summations over $\vec{l}$ and $\vec{k}$ are interchanged in (12), and we use the result

$$\frac{1}{N}\sum_{\vec{l}} e^{i\vec{k}\cdot\vec{l}} = \delta_{\vec{k}=0}.$$

The summation over $\vec{k}$ in (12) is now taken at the single point of $\vec{k}=0$. In order to examine the limit of $k \to 0$, we need to recall the small-k properties of these various vector transforms[19]

$$\lim_{k\to 0}\begin{cases} W_\mu^{e,i}(\vec{k}) = ik_\mu/k^2 + ik_\mu C_{e,i} + O(k^3), \\ T_{\mu\nu}^{e,i}(\vec{k}) = k_\mu k_\nu/k^2 - \tfrac{1}{3}\delta_{\mu\nu} + O(k^2). \end{cases} \tag{13}$$

The quantities C_e and C_i can be found from Ewald summations, and values for several lattice types are shown in Table II. There we give the dimensionless quantities $4\pi a C_{e,i}/V_0$ which depends only upon crystal structure. From the small-k limit (13) one can deduce the limiting behavior of the four $J_{NM}(\vec{k})$, and finally obtain the exact expression

$$\Sigma_2 = -\frac{4\pi}{V_0}\,\delta q\, q_B \frac{(C_e - C_i)(\bar{\alpha}_A - \bar{\alpha}_B)}{1+\tfrac{1}{3}(\bar{\alpha}_A + \bar{\alpha}_B)}.$$

TABLE II. C_e and C_i.

Crystal structure	$\frac{4\pi a C_e}{V_0}$	$\frac{4\pi a C_i}{V_0}$
NaCl	−1.5283	−0.3632
Zinc blende	−1.5283	−0.2673
CsCl	−0.9458	−0.2673

This is obviously simple to evaluate since one only needs to have the quantities $C_{e,i}$ in addition to the atomic polarizabilities. The same result, in both magnitude and sign, is obtained for the hole on either sublattice: in changing from halide to cation, the factor q_B changes sign, as does $(\bar{\alpha}_A - \bar{\alpha}_B)$.

Numerical results for both halide and cation holes are shown in Table III. The last three cesium compounds were calculated for the CsCl structure, while the others were calculated for the rocksalt structure. The sign of Σ_2 is usually positive, since it goes as $(\bar{\alpha}_A - \bar{\alpha}_B)$ and anion polarizabilities are mostly larger than those of cations. As discussed in Sec. I, the values of $E_b(H^-)$ and $E_b(A^+)$ are to be compared directly with the peak position of the hole band. A comparison with experimental values is deferred until Sec. IV. All hole bands in Table III are $p_{3/2}$ bands except for the 1s of lithium and the $d_{5/2}$ bands of silver. TKS polarizabilities[20] are used in constructing Table III. A similar table using JS polarizabilities[21] can be constructed using the values of Σ_{ML} in Table II and the equations for the other quantities. The actual hole energy $E_h = E_b - \Sigma_{ph}$, beneath the vacuum level, can only be found after computing the phonon self-energy Σ_{ph} and subtracting it from E_b. This is done in some cases, as described in the following section.

III. HOLE-PHONON INTERACTION

The role that phonons play in the optical properties of localized levels has been understood for nearly thirty years.[7,12-15] Here we adopt this standard model, and merely try to calculate the matrix elements for the hole-phonon interaction. These are used in Eqs. (1) and (2) for the hole self-energy and linewidth due to this interaction. The q integrals extend over the Brillouin zone, and are evaluated by the method of special points.

In the LHPI model, the matrix element for the hole-phonon interaction is derived from Eq. (4) for the ground-state energy. The change in energy is found as each ion is displaced from equilibrium $\vec{R}_j \to \vec{R}_j + \vec{Q}_j$. The displacements $\vec{Q}_j$ are assumed to be small, and the change in energy is only retained to linear terms in an expansion in $\vec{Q}_j$. There are thres types of terms which are produced by this procedure. First, there are the terms where the ion containing the hole is displaced. This has no linear interaction, because of the symmetric arrangement of the surrounding ions. Second, there is the displacement of the ions at $\vec{R}_j$ which has the point charge q_j. This is an important contribution which is

$$\delta E_g(Q_j) = \delta q \sum_{j\neq 0} q_j \left(\vec{w}(\vec{R}_{0j}) - \sum_m \vec{w}(\vec{R}_{0m}) \cdot \underline{\alpha}_m \cdot \underline{\phi}(\vec{R}_{jm}) + \sum_{nm} \vec{w}(\vec{R}_{0m}) \cdot \underline{\alpha}_m \cdot \underline{\phi}(\vec{R}_{mn}) \cdot \underline{\alpha}_n \cdot \underline{\phi}(\vec{R}_{nj}) - \cdots \right) \vec{Q}_j. \tag{14}$$

TABLE III. Core-hole energies (eV).

				Halide hole						Cation hole				
Salt	E_{MAD}	Σ_2	Σ_{ML}	$E_{elec}(H^-)$	E_A	$E_b(H^-)$	Σ_{ph}	$E_h(H^-)$	Σ_{ML}	$E_{elec}(A^+)$	E_{ip}	$E_b(A^+)$	Σ_{ph}	$E_h(A^+)$
LiF	12.529	+1.680	1.656	9.193	3.45	12.64	5.70	6.94	2.644	−16.852	75.62	58.77	4.99	53.78
LiCl	9.812	+2.055	1.916	5.841	3.61	9.45			3.202	−15.069	75.62	60.55		
LiBr	9.149	+2.055	1.911	5.183	3.36	8.54			3.216	−14.420	75.62	61.20		
LiI	8.389	+2.042	1.897	4.450	3.06	7.51			3.219	−13.650	75.62	61.97		
NaF	10.894	+0.694	1.441	8.759	3.45	12.21	3.92	8.29	1.846	−13.434	47.29	33.86	3.44	30.42
NaCl	8.924	+1.414	1.593	5.918	3.61	9.53	2.90	6.63	2.462	−12.800	47.29	34.49	2.33	32.16
NaBr	8.426	+1.519	1.618	5.298	3.36	8.65			2.566	−12.511	47.29	34.78		
NaI	7.776	+1.589	1.612	4.575	3.06	7.64			2.621	−11.985	47.29	35.30		
KF	9.413	−0.319	1.776	7.956	3.45	11.41			1.585	−10.679	31.81	21.13		
KCl	7.998	+0.611	1.543	5.845	3.61	9.46	2.09	7.37	1.920	−10.529	31.81	21.28	1.96	19.32
KBr	7.629	+0.803	1.518	5.305	3.36	8.67	1.96	6.71	2.021	−10.450	31.81	21.36	1.71	19.65
KI	7.123	+0.993	1.478	4.652	3.06	7.71	1.75	5.96	2.108	−10.225	31.81	21.58	2.02	19.56
RbF	8.924	−0.586	1.899	7.611	3.45	11.06	2.15	8.91	1.544	− 9.883	27.50	17.62	2.95	14.67
RbCl	7.648	+0.339	1.550	5.759	3.61	9.37	1.92	7.45	1.760	− 9.747	27.50	17.75	1.88	15.87
RbBr	7.343	+0.551	1.523	5.269	3.36	8.63	1.74	6.89	1.869	− 9.764	27.50	17.74	1.66	16.08
RbI	6.855	+0.762	1.443	4.650	3.06	7.71	1.61	6.10	1.926	− 9.543	27.50	17.96	1.44	16.52
AgF	10.230	−1.107	3.214	8.123	3.45	11.57			2.483	−11.606	21.48	9.87		
AgCl	9.074	+0.361	2.748	5.964	3.61	9.57			3.003	−12.438	21.48	9.04		
AgBr	8.715	+0.713	2.641	5.361	3.36	8.72			3.155	−12.583	21.48	8.90		
CsF	8.377	−0.961	2.201	7.137	3.45	10.59			1.604	− 9.020	25.10	16.08		
CsCl	7.109	−0.040	1.871	5.278	3.61	8.89			1.852	− 8.921	25.10	16.18		
CsBr	6.839	+0.204	1.807	4.828	3.36	8.19			1.902	− 8.944	25.10	16.16		
CsI	6.418	+0.475	1.698	4.245	3.06	7.31			1.919	− 8.812	25.10	16.29		

The third type of term is where the ion displacement occurs at the point $\vec{R}_m$ which is participating in the dielectric screening. This term is really just a phonon modulation of the dielectric function. We examined this term, but did not evaluate it because it appeared complicated and small. The hole-phonon interaction we evaluated is the series of terms in Eq. (14). It can be summed after we convert to reciprocal space using the lattice transforms in (7) and (9):

$$\delta E_g \equiv H_{h\text{-ph}} = -\frac{4\pi\delta q q_B}{V_0 N}\sum_{\vec{k}}\left[\vec{Q}_k^A\cdot\vec{J}_{AA}(\vec{k}) - \vec{Q}_k^B\cdot\vec{J}_{BA}(\vec{k})\right].$$

The standard definition[23] of $\vec{Q}_k$ then yields the final expression for the hole-phonon matrix element.

$$\vec{Q}_k^{A,B} = \left(\frac{\hbar}{2Nm^{A,B}}\right)^{1/2}\sum_\lambda \frac{\vec{e}_{\lambda\vec{k}}^{A,B}}{[\omega_\lambda(k)]^{1/2}}\,(a_{\vec{k}\lambda} + a_{\vec{k}\lambda}^\dagger),$$

$$M_\lambda(\vec{k}) = \frac{4\pi\delta q q_B}{V_0}\left(\frac{\hbar}{2N\omega_\lambda(\vec{k})}\right)^{1/2}\left(\frac{\vec{e}_\lambda^A\cdot\vec{J}_{AA}(\vec{k})}{(m^A)^{1/2}} - \frac{\vec{e}_\lambda^B\cdot\vec{J}_{BA}(\vec{k})}{(m^B)^{1/2}}\right).$$

The vectors $\vec{J}_{AA}(\vec{k})$ and $\vec{J}_{BA}(\vec{k})$ were evaluated by the procedure described in Sec. II.

A computer code was written to generate the phonon frequencies and polarization vectors $\vec{e}^{A,B}$. This is the type described in Ref. 24 where short-range interactions between first and second neighbors are described by adjustable force constants, and while long-range dipole forces were included by the quantities $\underline{T}^e$ and $\underline{T}^i$. The polarizable ion was simulated by an effective charge. This parameter, as well as the short-range force constants, was fitted to the measured phonon frequencies at the zone center and at the X point. This method seems to be a simple and accurate interpolation scheme for phonon states, but requires a previous measurement of phonon frequencies by neutron or x-ray scattering. Calculations were done for ten cases where we found such data: LiF,[25] NaF,[26] NaCl,[27] KCl,[28,29] KBr,[30] KI,[31] RbF,[32] RbCl,[32] RbBr,[33] and RbI.[34]

The hole self-energies Σ_{ph} from this interaction are temperature independent, and are shown in Table III for halide and cation holes. The numerical values are larger than expected, and are larger

than the Mott-Littleton energy. This shows the Mott-Littleton argument that the phonon self-energy is small and can be neglected is incorrect. A previous estimate of this self-energy was given by Citrin, Eisenberger, and Hamann (CEH),[7] whose formulas for the self-energy and linewidth are

$$\Sigma_{ph}=e^2(6/\pi V_0)^{1/3}(1/\epsilon_\infty - 1/\epsilon_\infty),$$
$$\Delta(T)=2.35(\hbar\omega_{LO}\Sigma_{ph})^{1/2}[\coth(\beta\hbar\omega_{LO}/2)]^{1/2}. \quad (15)$$

This is based upon a simple model whereby the polar interaction to LO phonons provides the only interaction. Their formula for Σ_{ph} predicts values systematically lower than ours. In fact, we agree much better if their numbers are multiplied by a factor of 2. Our calculation also predicts different self-energies for halide and cation holes, whereas they would predict the same.

CEH presented linewidth data as a function of temperature for three potassium halides, and we were able to calculate for two of these, KCl and KI. The comparison of theory and experiment for cation holes is shown in Fig. 2. The lines marked "theory" are our results, and the CEH theory of Eq. (15) is also shown. The solid points are the raw data of CEH, and the open points are their corrected data. These corrections include instrumental resolution, and other contributions to the linewidth, so that the corrected data represented just the phonon contribution to the linewidth. The upturn in the raw data at low T is an effect of sample charging, which they also try to correct.

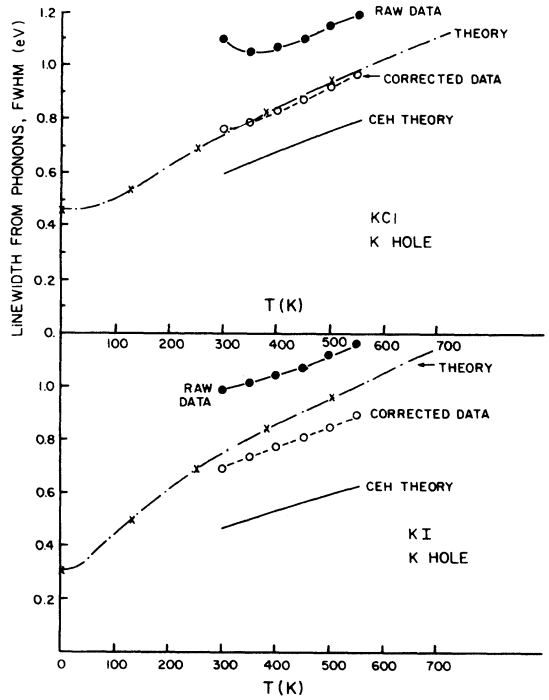

FIG. 2. The phonon contribution to the x-ray photoemission spectroscopy linewidth (FWHM) from potassium core states. The raw and corrected data are from Citrin, Eisenberger, and Hamann in Ref. 7. Their theory curve is also shown. The present theory is the dot-dash line which extends zero temperature. It agrees well with the experimental phonon contribution to the linewidth, which is the corrected datum.

The agreement between our theory and their experiment is obviously excellent for KCl. The agreement for KI is not as spectacular, but still satisfactory. We conclude that the agreement between theory and experiment is satisfactory, and shows that the standard model of Huang and Rhys does explain the phonon part of the linewidth in photoemission, in agreement with the conclusion of CEH.

For each of the ten solids, the linewidth Eq. (2) was evaluated at five different temperatures for both halide and alkali holes. Rather than present all of this output, we sought a simple interpolation scheme for presenting the temperature dependence. Guided by the CEH formula (15) for $\Delta(T)$, we tried

$$\Delta(T)=\Delta_0[\coth(\beta\hbar\omega_1/2)]^{1/2}. \quad (16)$$

This worked amazingly well in describing the temperature dependence, when $\hbar\omega_1$ is treated as an adjustable parameter. One can accurately fit all five temperature points, equally spaced between 1 and 500 K, by just two constants, where Δ_0 is the zero-temperature limit of $\Delta(T)$. The values of Δ_0 and $\hbar\omega_1$ are shown in Table IV for the ten solids. The dot-dashed curve in Fig. 3 was actually calculated with the interpolation formula (16), while the x points were the full computer calculation with the integral over the Brillouin zone. We have checked that the interpolation procedure works equally well for all 20 cases, i.e., halide and cation hole in the ten solids.

The unexpected feature of the calculations is that the linewidth has a different temperature dependence for the halide and alkali holes in the same solid. This is shown by the different values of $\hbar\omega_1$ found in the two cases. Obviously different phonons affect each hole. This difference is most pronounced in KI, while in KCl the difference is negligible. This raises the question as to whether the energy $\hbar\omega_1$ can be associated with any particular phonon. In Table IV we have also listed the LO-phonon energies at the Γ point and also at the X point. The Γ-point values are obviously much higher than $\hbar\omega_1$ so that they do not correspond to the observed temperature dependence. Better agreement is found with the values of $\hbar\omega_{LO}$ at the X point. In all of the alkali halides, the LO-phonon energy has its highest value at the Γ point, and falls rapidly in value as k is increased in any di-

TABLE IV. Phonon linewidths FWHM in eV.

	$\Delta(T) = \Delta_0 [\coth(\frac{1}{2}\beta\omega_1)]^{1/2}$					
	Halide hole		Alkali hole			
Salt	Δ_0	$\hbar\omega_1$	Δ_0	$\hbar\omega_1$	$\hbar\omega_{LO}(\Gamma)$	$\hbar\omega_{LO}(X)$
LiF	1.426 eV	0.0690 eV	1.180 eV	0.0538 eV	0.0816	0.0568
NaF	0.900	0.0404	0.881	0.0446	0.0524	0.0353
NaCl	0.624	0.0259	0.538	0.0245	0.0324	0.0240
KCl	0.465	0.0201	0.455	0.0207	0.0265	0.0195
KBr	0.414	0.0169	0.355	0.0145	0.0207	0.0167
KI	0.364	0.0146	0.305	0.0088	0.0176	0.0140
RbF	0.492	0.0221	0.644	0.0270	0.0356	0.0226
RbCl	0.380	0.0146	0.419	0.0183	0.0214	0.0166
RbBr	0.331	0.0122	0.324	0.0123	0.0161	0.0123
RbI	0.292	0.0102	0.262	0.0093	0.0130	0.0105

rection away from $k = 0$. Since there is more phase space at large k, then zone-edge values of $\hbar\omega_{LO}$ are more important than the value at the zone center. Similar values for $\hbar\omega_{LO}$ are found for all of the zone-edge points, and are similar to the nearly constant values of $\hbar\omega_{TO}$ throughout the zone. By studying the polarization vectors it appears that LA and LO phonons near the zone edge provide the important temperature dependence to the linewidth. The Fröhlich polaron model which is the basis for the CEH formula (15) is not accurate in this region.

IV. RESULTS AND DISCUSSION

The phonon results were discussed in the preceding section. Now the theory for the core binding energies will be compared with experiment. It was discussed in Sec. I and illustrated in Fig. 1 that the phonon self-energy does not affect the observed binding energy of the photoemitted electrons. Instead, the phonon processes impart a Gaussian line shape to the spectra, whose peak is at the value E_b calculated in the absence of phonon processes. Thus we shall compare the values of $E_b(H^-)$ and $E_b(A^+)$ derived in Table III with the available experimental data. This comparison is shown in Table V.

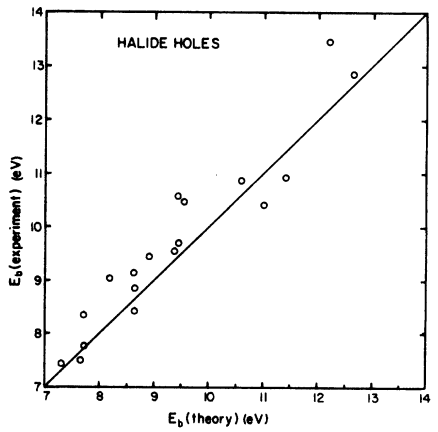

FIG. 3. A graphical comparison between theory and experiment for photoemission binding energies for halide holes.

We have chosen three sets of data for comparison: Citrin and Thomas,[1] Poole *et al.*,[2] and Pong *et al.*[3-6] Both Poole *et al.* and Pong *et al.* report the binding energies of valence-band peaks, and they can be approximately deduced from Citrin and Thomas. A comparison of the several sets of experimental results on the same hole rarely show agreement within 1 eV. This is undoubtedly due to the presence of sample charging during the experiment, which all experimentalists complain about. The agreement between theory and experiment is quite good: usually within 1 eV, which is the variation among the different sets of data. The comparison is given visually in Fig. 3, which plots points for halide holes according to the theoretical and experimental values: the experimental point is the average of the data set. Perfect agreement would have all points on the solid line. In fact, rather good agreement is obtained since most points are within a few tenths of an electron volt, which is about the experimental uncertainty. Our conclusion is that the localized-hole point-ion (LHPI) model describes rather accurately the photoemission peaks for holes in alkali halides.

The tables also present the same calculations for the three silver halides with the rocksalt structure. In Table III it is shown that the halide p hole and the silver d hole have nearly the same energy. This is in accord with numerous photoemission measurements[35-37] which show these holes at the same energy, and strongly hybridized. The observed valence bands are 6-eV wide, which is

TABLE V. $E_c(H^-)$ and $E_c(A^+)$ in eV.

Salt	Halide hole				Alkali hole			
	Poole[a]	Pong[b]	Citrin[c]	Theory	Poole[a]	Pong[b]	Citrin[c]	Theory
LiF	12.85			12.64				58.77
LiCl	10.80	10.6	10.3	9.45			60.7	60.55
LiBr	9.80			8.54				61.20
LiI				7.51				61.97
NaF	11.88	13.0	15.4	12.21			36.9	33.86
NaCl	10.45	10.0	10.9	9.53			36.3	34.49
NaBr	9.22		9.2	8.65			35.7	34.78
NaI			7.5	7.64			35.5	35.30
KF	10.63	11.2		11.41	21.23			21.13
KCl	9.60	9.6	9.9	9.46	22.10		21.8	21.28
KBr	8.83			8.67	21.97		20.5	21.36
KI	8.18	8.5		7.71	22.08		20.0	21.58
RbF	9.98	10.8		11.06	17.72	17.5		17.62
RbCl	9.35	9.5	9.8	9.37	18.65	18.0	18.6	17.75
RbBr	7.94	8.9		8.63	17.79	18.2		17.74
RbI	7.33	8.2		7.71	18.11	18.4		17.96
CsF	10.03	10.0	12.6	10.59	15.30	14.5	15.3	16.08
CsCl	9.15	9.0	10.1	8.89	15.85	14.5	15.2	16.18
CsBr	8.41	8.2	10.5	8.19	15.75	14.6	15.1	16.16
CsI	7.60	7.0	7.7	7.31	15.70	14.5	14.1	16.29

[a] Poole *et al.*, Ref. 2.
[b] Pong *et al.*, Refs. 3–6.
[c] Citrin and Thomas, Ref. 1.

proof that band structure is important for these solids. The LHPI model should certainly *not* be applied to describing the photoemission from these hybridized bands. However, as noted by Tejeda *et al.*,[37] this hybridization leaves some d orbitals unaffected, and holes in them are localized. The LHPI model should apply to these holes, which appear as sharp peaks in the photoemission with a binding energy of 9.0–9.5 eV in AgCl and AgBr. This is exactly where we predict the d holes to be in our model, as shown in Table III. It appears that the LHPI model can be successfully applied to the d-band holes which do not participate in the hybridization.

An accurate calculation of photoemission thresholds for metals requires the inclusion of the surface dipole layer. Euwema and Surratt[11] have shown how to include such effects in ionic solids. For rocksalt lattices, one would expect a surface dipole for the (111) face, but would not for the (100) or (110) faces.

Another approximation of the LHPI model is the neglect of short-range repulsive forces between the ions. Repulsive forces enter the present model in two ways. The first is the change in the ionization potential of the free ion due to the compression upon the ion by its immediate neighbors. Jennison and Kunz[38] have shown that the ions are spherical except at the compression regions. The second way repulsive forces enter into the model is through the hole-phonon interaction. Again we only need to know how the hole changes the repulsive force constants. This will affect the phonon-induced linewidth, and self-energy. These factors are difficult to estimate.

Citrin and Thomas[1] gave an estimate of the Born-Mayer repulsive energy, and its contribution to threshold energies in photoemission. We believe their estimates are too large for the following reason. They used the standard form of the repulsive energy

$$E_{\mathrm{Rep}} = 6B\{\beta_{AC} + \beta_{CC}\exp[2r_C - \sqrt{2}(r_C + r_A)]/\rho + \beta_{AA}\exp[2r_A - \sqrt{2}(r_C + r_A)]/\rho\},$$

$$\beta_{ij} = 1 + Z_i/n_i + Z_j/n_j .$$

Here r_C and r_A are the cation and anion radii, B and ρ are hardness and strength parameters, and Z and n are the valence (=+1) and number of outer electrons (=8). This repulsive-energy contribution

to the ground-state energy of an alkali halide has a typical value of 1 eV. They assumed that during a photoemission event all of the repulsive energy of an ion vanishes, and the repulsive energy is imparted to the photoemitted electron. They obtain an estimated 1-eV contribution to the repulsive energy of the electron. We think that the ion which remains behind to host the hole still has repulsive energy. Rather than assign all of the repulsive energy of the ion to the photoemitted electron, it seems reasonable to estimate the change in repulsive energy due to the loss of a single electron. The Born-Mayer theory provides a convenient way of doing this, since one can estimate the change in repulsive energy due to Z changing by plus one and n changing by minus one. The result for cations and anions is

$$\delta E^{C}_{\mathrm{Rep}} = 6B\,\delta(Z/n) \times \{1+2\exp[2r_C - \sqrt{2}\,(r_C+r_A)]/\rho\},$$

$$\delta E^{A}_{\mathrm{Rep}} = 6B\,\delta(Z/n) \times \{1+2\exp[2r_A - \sqrt{2}\,(r_C+r_A)]/\rho\}.$$

The factor $\delta(Z/n)$ equals $-\frac{9}{56}$ for cations and $-\frac{1}{8}$ for anions. Using the parameters of Citrin and Thomas for NaCl, one finds that the change in repulsive energy is -0.11 eV for anions, and -0.12 eV for cations. Both values are smaller than the other energy terms we have calculated, and small enough to be neglected. Thus we find that the repulsive-energy contribution to the photoemission energy is small, contrary to the conclusion in Ref. 1.

The above discussion of repulsive contributions assumed that the ions were frozen at their lattice sites. The change in repulsive energy will cause a change in the local configuration of neighboring ions around the hole. This rearrangement will not alter the energy of the photoemitted electron, which should be calculated using the frozen lattice approximation. The argument for this approximation is that the electron leaves the site far too rapidly for the slow response of the ions. We discussed in Sec. III that the phonon self-energies do not affect the peak energies in photoemission, which also happens because the ions do not respond sufficiently rapidly. The same argument shows that the ion response to the change in local repulsion also occurs on the same slow time scale, and does not influence electron threshold energies. Thus we conclude that the local ion repulsion makes a negligible contribution to the energies of the photoelectrons.

ACKNOWLEDGMENTS

I wish to thank Professor W. L. Schaich for suggesting the method of special-points integration. The research was supported by the Air Force Office of Scientific Research Grant No. 76-3106.

[1] P. H. Citrin and T. D. Thomas, J. Chem. Phys. 57, 4446 (1972).
[2] R. T. Poole, J. G. Jenkin, J. Liesegang, and R. C. G. Leckey, Phys. Rev. B 11, 5179 (1975).
[3] W. Pong and J. A. Smith, Phys. Rev. B 7, 5410 (1973).
[4] W. Pong and J. A. Smith, in *Vacuum Ultraviolet Radiation Physics*, edited by E. Koch, R. Haensel, and C. Kunz (Pergamon, New York, 1974), p. 383.
[5] W. Pong and J. A. Smith, Phys. Rev. B 9, 2674 (1974).
[6] C. S. Inouye and W. Pong, Phys. Rev. B 15, 2265 (1977).
[7] P. Citrin, P. Eisenberger, and D. Hamman, Phys. Rev. Lett. 33, 965 (1974).
[8] N. F. Mott and M. J. Littleton, Trans. Faraday Soc. 34, 485 (1938).
[9] D. J. Chadi and M. L. Cohen, Phys. Rev. B 8, 5747 (1973).
[10] A. B. Kunz, Phys. Rev. B 6, 606 (1972); 12, 5890 (1975).
[11] R. N. Euwema and G. T. Surratt, J. Phys. Chem. Solids 36, 67 (1975).
[12] K. Huang and A. Rhys, Proc. R. Soc. London, Ser. A 204, 406 (1950); J. J. Markham, Rev. Mod. Phys. 31, 956 (1959).
[13] L. G. Parratt, Rev. Mod. Phys. 31, 616 (1959), see footnote 108.
[14] M. Lax, J. Chem. Phys. 20, 1752 (1952).
[15] C. B. Duke and G. D. Mahan, Phys. Rev. 139, A1965 (1965).
[16] C. E. Moore, *Atomic Energy Levels*, NBS Circular No. 467 (U.S. GPO, Washington, D. C., 1949).
[17] R. S. Berry and C. W. Reimann, J. Chem. Phys. 38, 1540 (1963).
[18] G. D. Mahan, Phys. Rev. 153, 983 (1967).
[19] G. D. Mahan and R. M. Mazo, Phys. Rev. 175, 1191 (1968).
[20] J. R. Tessman, A. H. Kahn, and W. Shockley, Phys. Rev. 92, 890 (1953).
[21] S. S. Jaswal and T. P. Sharma, J. Phys. Chem. Solids 34, 509 (1973).
[22] F. K. DuPré, R. A. Hutner, and E. S. Rittner, J. Chem. Phys. 18, 379 (1950).
[23] A. A. Maradudin, E. W. Montroll, G. H. Weiss, and I. P. Ipatova, *Theory of Lattice Dynamics in the Harmonic Approximation* (Academic, New York, 1971), Chap. 2.
[24] M. B. Haxton, Phys. Status Solidi B 78, 259 (1976); 86, 661 (1978).
[25] G. Dolling, H. G. Smith, R. M. Nicklow, P. R. Vijayaraghvan, and M. K. Wilkinson, Phys. Rev. 168, 970 (1968).
[26] W. Buyers, Phys. Rev. 153, 923 (1967).

[27]R. E. Schmunk and D. R. Winder, J. Phys. Chem. Solids 31, 131 (1970).
[28]J. R. D. Copley, R. W. Macpherson, and T. Timusk, Phys. Rev. 182, 965 (1969).
[29]G. Raunio and L. Almqvist, Phys. Status Solidi 33, 209 (1969).
[30]A. D. B. Woods, B. N. Brockhouse, R. A. Cowley, and W. Cochran, Phys. Rev. 131, 1025 (1963). They also report results for NaI, but our phonon interpolation did not work for this case, so it was not included.
[31]G. Dollling, R. A. Cowley, C. Schittenholm, and I. M. Thorson, Phys. Rev. 147, 577 (1966).
[32]G. Raunio and S. Rolandson, J. Phys. C 3, 1013 (1970).
[33]S. Rolandson and G. Raunio, J. Phys. C 4, 958 (1971).
[34]G. Raunio and S. Rolandson, Phys. Status Solidi 40, 749 (1970).
[35]M. G. Mason, Phys. Rev. B 11, 5094 (1975).
[36]R. S. Bauer and W. E. Spicer, Phys. Rev. B 14, 4539 (1976).
[37]J. Tejeda, N. J. Shevchik, W. Braun, A. Goldmann, and M. Cardonna, Phys. Rev. B 12, 1557 (1975).
[38]D. W. Jennison and A. B. Kunz, Phys. Rev. B 13, 5597 (1976).